

Steerable Phased Array Antennas Using Single-Crystal YIG Phase Shifters—Theory and Experiments

H. How, Ping Shi, C. Vittoria, E. Hokanson, M. H. Champion, Leo C. Kempel, *Senior Member, IEEE*, and Keith D. Trott, *Senior Member, IEEE*

Abstract—A phased array antenna containing four linear microstrip patch elements has been fabricated and tested. The elements were fed through single-crystal yttrium-iron-garnet (YIG) phase shifters. By varying the bias magnetic field, the input phases to the antenna elements can thus be tuned, resulting in steering of the radiation beam in one dimension. Measurements compared reasonably well with calculations.

Index Terms—Ferrite phase shifter, magnetic microwave device, microstrip device, steerable phased array.

I. INTRODUCTION

MICROWAVE and millimeter-wave (MMW) devices and systems are becoming increasingly important for both defense and commercial applications. Phase shifters are the building blocks of high-performance phased array radars and communications systems. As contrasted to mechanically tuned devices, the phases of electrically tuned phase shifters use frequency agile materials whose electronic properties can be varied via the application of a voltage, a magnetic field, or a current [1]. In varactor diode phase shifters a varactor diode is used as a variable-capacitance element [2]. This variable capacitance is obtained through a voltage-tuned capacitance of the diode under a reverse-bias condition [3]. For a ferroelectric phase shifter the permittivity for wave propagation is controlled by a bias electric voltage [4], and for a ferrite phase shifter the permeability is controlled by a bias magnetic field or a bias current in a solenoid coil [5].

While it is possible to fabricate a phase shifter at low frequencies by using a ferroelectric substrate, say, below 5 GHz [6], it is not very feasible if the frequency is increased to *X*-band or beyond, since ferroelectric materials are generally lossy at high frequencies [7]. At *X*-band and above insertion losses are lower in ferrite substrates [8]. Furthermore, a ferrite phase shifter can

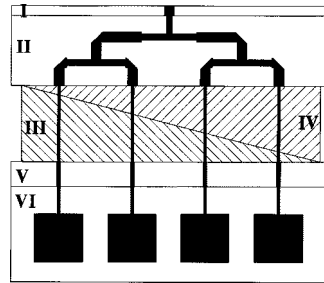


Fig. 1. Layout of the phased array antenna.

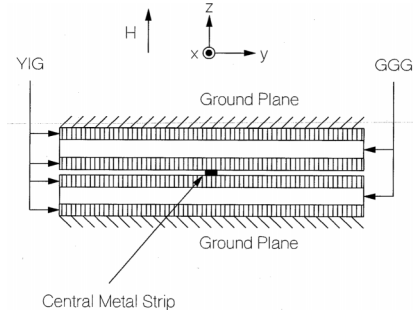


Fig. 2. Cross-sectional view of the ferrite phase shifter.

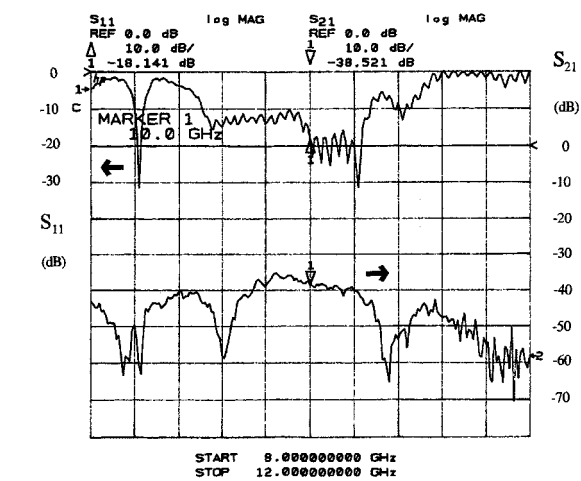


Fig. 3. The measured reflection S_{11} and transmission S_{21} data of the fabricated phased array antenna.

Manuscript received August 5, 1999. This work was supported by AFOSR/NM.

H. How is with ElectroMagnetic Applications, Inc., Boston, MA 02109 USA.

P. Shi and C. Vittoria are with Northeastern University, Boston, MA 02115 USA.

E. Hokanson is with Trans-tech, Inc., Adamstown, MD 21710 USA.

M. H. Champion is with the USAF Rome Laboratory, Hansom, MA 01731 USA.

L. C. Kempel is with Michigan State University, East Lansing, MI 48824 USA.

K. D. Trott is with Mission Research Corporation, FL 32580 USA.

Publisher Item Identifier S 0018-9480(00)07392-0.

support high power [9] as compared to a varactor diode operating under the reverse-bias condition [3].

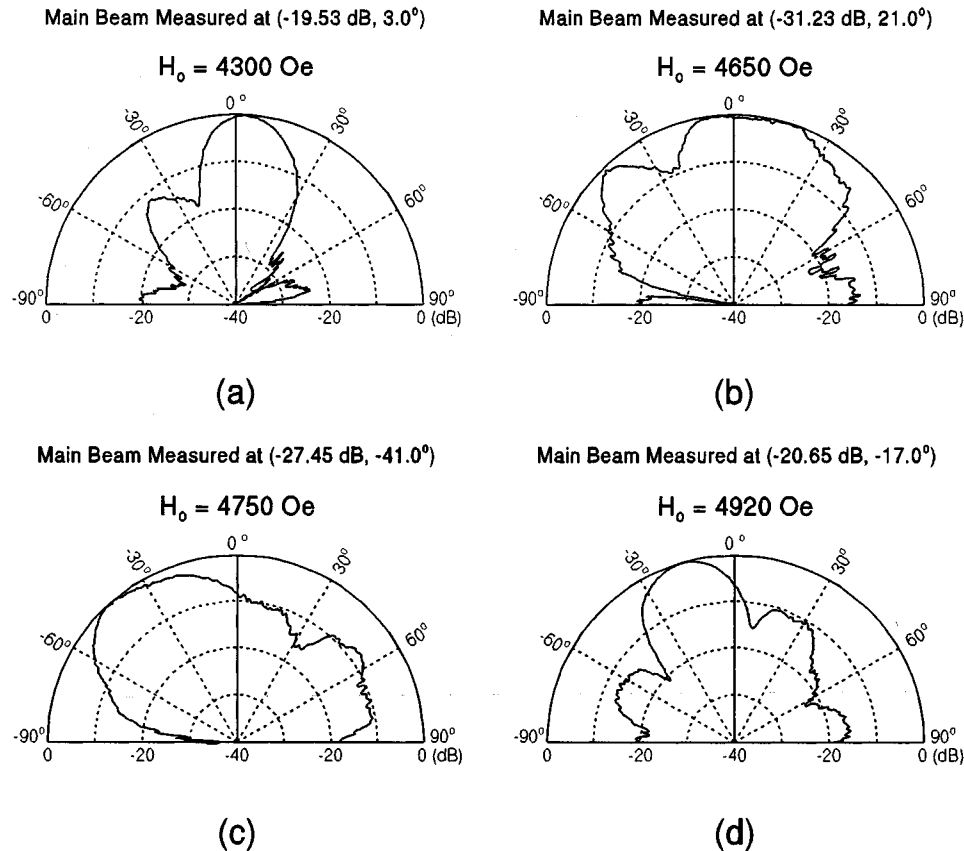


Fig. 4. Measured radiation patterns for the bias field: (a) $H_o = 4300$ Oe, (b) 4650 Oe, (c) 4750 Oe, and (d) 4920 Oe.

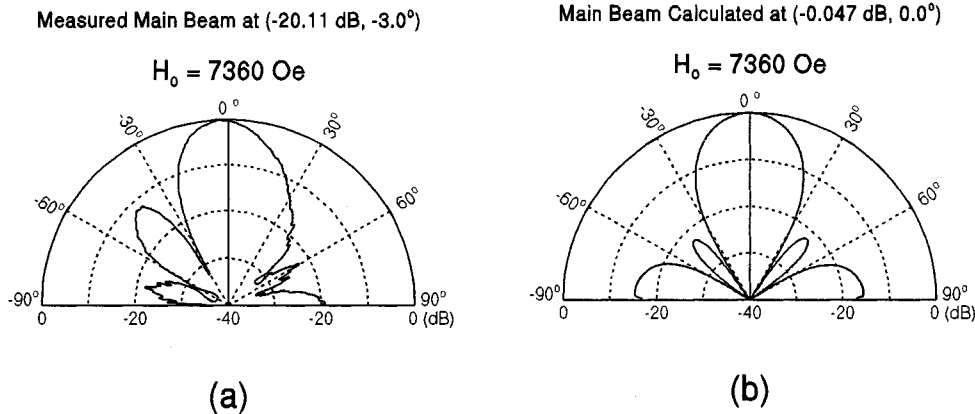


Fig. 5. (a) Measured and (b) calculated radiation patterns for $H_o = 7360$ Oe. At this bias field strength the permeability of the substrate is close to 1, giving rise to radiation patterns of a dielectric substrate.

In this paper we report the performance of a linear phased array antenna at *X*-band using single-crystal yttrium-iron-garnet (YIG) as the frequency agile material adjusting the input phase of the radiating elements. The array contains four square patches, connected to four stripline feeders with equal power. The feeders include YIG phase shifters whose output phases can be progressively varied via an external magnetic field applied normal to the array substrate [10]. This results in steering of the radiation beam from the antenna array in one dimension.

The difficulty in using a ferrite substrate at *X*-band frequencies is that the bias magnetic field requires a magnitude at least several thousand oersteds to effectively change the permeability of the substrate. In order to practically use a ferrite substrate the bias field is thus divided in two parts: the permanent part and the variable part. The permanent part of the bias field is furnished by using a permanent magnet, providing a constant background for magnetic biasing. The variable bias field is then superimposed to the permanent part, resulting in local variation of the bias field near its permanent field value. The variable field re-

quires only a small magnitude in comparison to the permanent field, which can then be conveniently obtained by using a solenoid coil.

In order to reduce the bias current in the solenoid coil, and hence to enhance the switching speed of the phase shifter and to lower power dissipation, the magnitude of the variable bias field shall be kept as a minimum. For this purpose we desire to operate a ferrite phase shifter near ferromagnetic resonance (FMR). In the vicinity of FMR the permeability of the ferrite material is a sensitive function of the bias field, and a slight change in the bias field can result in a significant change in permeability [10]. However, the price to pay is that when FMR is approached, wave propagation in the ferrite material becomes very lossy. To overcome this difficulty we have demonstrated that it is possible to operate a ferrite phase shifter near FMR without causing much magnetic loss if the ferrite material exhibits a narrow FMR linewidth [11].

Due to the very narrow FMR linewidth of single-crystal YIG it is an ideal material to be used for microwave phase-shifters at *X*-band. The linewidth of single-crystal YIG is about 0.5 Oe at *X*-band. We have fabricated and tested an *X*-band stripline phase shifter using single-crystal YIG thick films as the substrate material [11]. We found that at 10 GHz the phase shifter, which is of a quarter-wave length in the absence of a bias magnetic field, produced a phase change of 120° in the transmitted signal when the internal field was varied 3440–3720 Oe. The accompanying change in insertion loss was 0.5–0.4 dB [11].

In this paper we report the performance of a phased array at *X*-band using single-crystal YIG phase shifters as the phase tuning elements. The array contains four linear rectangular microstrip patches. We found that sensitive beam steering occurs near FMR at 4750 Oe of the applied magnetic field. However, useful radiation patterns result only when the YIG material is biased at the knee above FMR giving rise to narrow-beam radiation with insignificant attenuation (or large radiation efficiency). This corresponds to about a beam-steering angle of 15° for the bias field varying 4920–5270 Oe. Larger steering angles are obtainable if longer phase shifter lines are used.

The performance of the phase shifters has been analyzed numerically by using the transfer-matrix theory in a transmission line structure involving multilayers. The transfer-matrix theory is usually used to translate the transverse electromagnetic boundary conditions occurring at one layer interface to another, expressing the continuity equation in the spectral domain [12], [13]. A surface impedance matrix was first defined at a layer interface. The impedance matrices associated with an imperfect metal ground plane and an open half-space were then derived. While a conventional transfer matrix correlates the tangential components of the rf-electromagnetic field over one layer thickness [14]–[16], the transformation of surface impedance can be thereof defined, transforming the surface impedance matrix also over one layer thickness. When two transfer matrices are multiplied, the associated impedance transformation are compounded so that the resultant transformation is isomorphic to the multiplication of the two transfer matrices. As such, the surface impedance at the outermost surfaces of the layered structure can be translated to the plane(s) containing circuit inhomogeneities from which the (normal) metal boundary

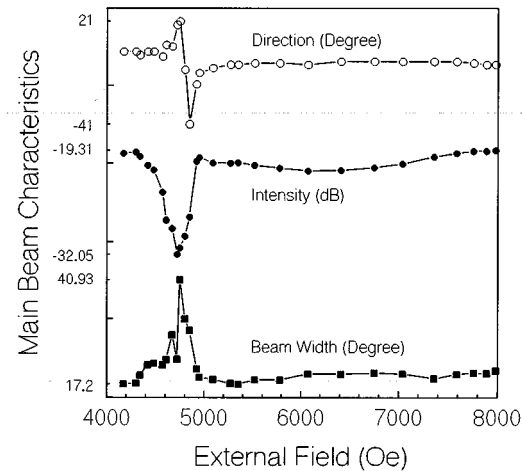


Fig. 6. Calculated main-beam properties plotted as a function of the external bias field: beam direction, intensity, and beam width.

conditions can be applied and solved. Detailed formulation and calculations of this kind will be published elsewhere.

After the wave propagation constants and the impedances of the ferrite transmission lines have been solved using the spectral domain analysis, the phase shifting properties of the phase shifters employed in the fabricated phased array are therefore determined. By using the transmission-line theory and the cavity model [17], the radiation pattern from the array can thus be calculated. Calculations compared reasonably well with measurements.

II. RESULTS

Fig. 1 shows the layout of the fabricated antenna array. In Fig. 1 six regions are distinguished. Region I is of a width 2.5 in and a length 0.0764 in, containing a stripline of impedance 50 Ω using air as the substrate/superstrate material. The stripline is connected to an coax (OSM) launcher for microwave input. Region II, 2.5×0.570 in², contains stripline power splitters, and the input microwave power is divided into four equal parts with little reflection. In Region II duroid (dielectric constant 2.2, thickness 0.031"; Rogers, Chandler, AZ) is used as the substrate/superstrate material. Region V, 2.5×0.199 in², includes four stripline transformers using the same duroid material as the substrate and the superstrate, and Region VI, 2.5×0.75 in², contains four microstrip patches attached with feeders deposited on the same piece of the substrate extended from Region V. No superstrate is used in Region VI, radiating energy away from the antennas allowing measurements to be taken directly above Region VI. The microstrip patches are of a square geometry with dimension 0.388×0.388 in². The stripline/microstrip circuit as well as the six regions shown in Fig. 1 has been drawn in scale.

In Fig. 1 Region IV contains frequency agile material used to construct stripline phase shifters, and Region III is for phase compensation. That is, we require these two regions to have the same dielectric constant so that equal phase results at the input of the patch antennas in the absence of a bias magnetic field. The boundary between Regions IV and III is linearly tapered so as to provide progressive phase changes when the permeability of

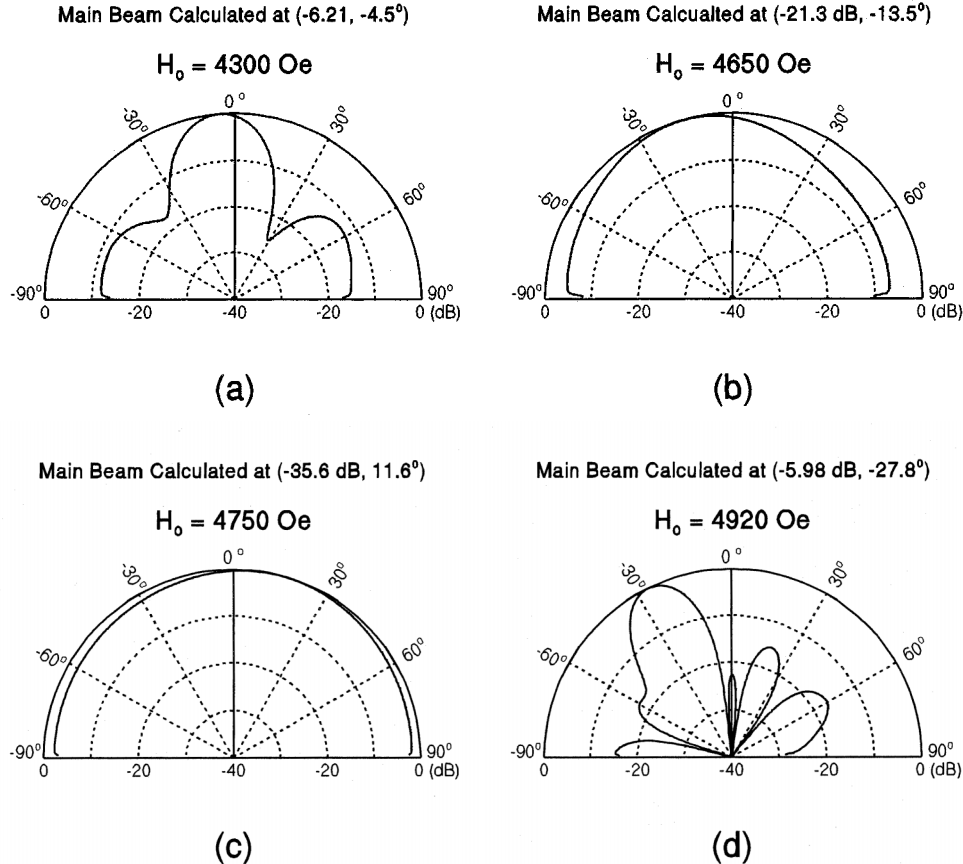


Fig. 7. Calculated radiation patterns for the bias field: (a) $H_o = 4300$ Oe, (b) 4650 Oe, (c) 4750 Oe, and (d) 4920 Oe.

the substrate/superstrate of Region IV is varied. A bias field is applied normal to the substrate/superstrate surface, whose magnitude can be varied 4000–8000 Oe. The magnetic field is supplied by using a pair of neodymium permanent magnets ($2 \times 2 \times 1$ in 3) and the bias field can be varied by adjusting the gap distance separating the yoke arms connected to the permanent magnets. The dielectric constant of the dielectric material used in Region III is 14 (Trans Tech, Adamstown, MD). The dimension of Region III plus Region IV is 2×0.616 in 2 .

In Region IV we use single-crystal YIG/GGG/YIG as the frequency agile material, and a cross-sectional view of the corresponding stripline geometry is shown in Fig. 2. The YIG/GGG/YIG material was purchased from Airtron, Charlotte, NC. The YIG films are of a nominal thickness of 100 μ m, which were epitaxially grown along the $\langle 111 \rangle$ direction on both sides of a crystal GGG substrate (thickness 20 mil and dielectric constant 14.7). The YIG films are characterized by the following parameters: saturation magnetization $4\pi M_s = 1750$ G, dielectric constant $\epsilon_f = 14.7$, anisotropy field $H_A = 82$ Oe, and an FMR line-width $\Delta H \approx 0.5$ Oe at 10 GHz. The dielectric loss-tangent for both YIG and GGG materials is 0.0002.

The circuit of Fig. 1 was characterized using a vector network analyzer, HP-8510B. As shown in Fig. 3 the reflection data, S_{11} , indicate that the fabricated antenna array is of a bandwidth extending 9.1–10.5 GHz. The transmission data S_{21} was measured

using a waveguide horn antenna placed 5 ft above the antenna array (on top of Region VI, Fig. 1). No shielding was applied during the transmission measurement and the measured S_{21} data of Fig. 3 include multiple-path reflections.

The radiation pattern of the antenna array was measured in an anechoic chamber located at Rome Laboratory, Hanscom, MA. Fig. 4(a)–(d) shows the measured radiation patterns that the phase-shifter circuit was biased under several magnetic field values below, near, and above ferrimagnetic resonance (FMR). Fig. 5(a) shows the measured radiation pattern when the YIG films were biased far beyond FMR so that they behaved like dielectric materials. That is, when biased far beyond FMR, the effective permeability of YIG films approaches unity. Fig. 5(b) shows the calculated radiation pattern of the array at the same bias field strength to be discussed shortly. The measured intensity and location of the main-beam radiation are also indicated in Fig. 4(a)–(d) and Fig. 5(a). The properties of the measured main-beam radiation are summarized in Fig. 6, where the location, the intensity, and the beam width are plotted as a function of the applied bias-field strength H_o . From Fig. 6, also from Fig. 4(d), it is seen that useful radiation occurs when the bias field H_o is varied 4920–5270 Oe, resulting in a beam steering angle of 15° without causing much beam broadening and attenuation.

The calculated radiation patterns are shown in Fig. 7(a)–(d) and Fig. 5(b), corresponding to the same bias fields of the measurements shown in Fig. 4(a)–(d) and Fig. 5(a), respectively.

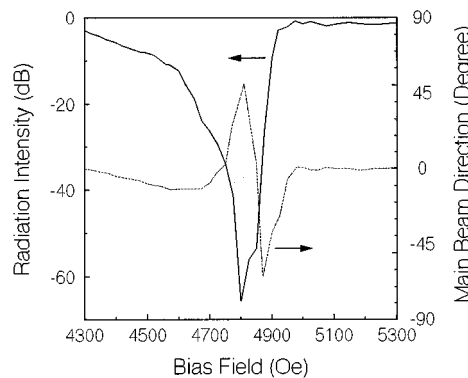


Fig. 8. Calculated main-beam properties plotted as a function of the external bias field: beam, direction, and intensity.

The calculated main beam radiation, the intensity and location, is also indicated in Fig. 7(a)–(d) and Fig. 5(b), referenced with respect to that when the ferrite substrate/superstrate is fully saturated, as closely represented by the pattern shown in Fig. 5(b). The calculated properties of the main-beam radiation, the intensity, and the location are plotted in Fig. 8 as a function of the bias-field strength, H_o . Comparing Fig. 4(a)–(d) and Fig. 5(a) with Fig. 7(a)–(d) and Fig. 5(b), we conclude that calculations compare reasonably well with measurements, especially when the bias field was applied far beyond ferrimagnetic resonance, Fig. 5(a) and (b), corresponding to the case of a dielectric substrate/superstrate. However, we note that discrepancy occurs near ferrimagnetic resonance (FMR) where the calculated radiation intensity is weaker than was measured. When FMR is approached, wave propagation becomes quasi-singular, resulting in significant truncation errors in the calculations.

III. CONCLUSIONS

We conclude that practical phased array antennas operating at X -band can be fabricated using single-crystal YIG materials characterized by a narrow FMR linewidth. While the transmission phase can be sensitively tuned by applying a bias magnetic field, the insertion loss occurring at the phase shifters can be retained at a relatively constant low level. In addition, it is only necessary to bias the YIG-film material with a small variable field of magnitude ± 100 Oe, which can be conveniently obtained by using a solenoid coil; the rest of the bias field can be supplied by permanent magnets serving as a background. Except for the FMR region, the measured radiation patterns compared reasonably well with experiments.

REFERENCES

- [1] A. F. Harvey, *Microwave Engineering*. New York, NY: Academic, 1963.
- [2] G. Gonzales, *Microwave Transistor Amplifiers*. Englewood Cliffs, NJ: Prentice-Hall, 1984.
- [3] S. M. Sze, *Physics of Semiconductor Devices*. Murray Hill, NJ: Wiley-Interscience, 1981.

- [4] F. De Flaviis, O. M. Stafudd, and N. G. Alexopoulos, "Planar microwave integrated phase shifter design with high purity ferroelectric materials," *IEEE Trans. Microwave Theory Tech.*, vol. 45, pp. 963–969, 1997.
- [5] G. P. Rodrigue, "Magnetic materials for millimeter wave applications," *IEEE Trans. Microwave Theory Tech.*, vol. MTT-11, pp. 351–356, 1963.
- [6] R. Babbit and W. Drach, "Ferroelectric phase shifters for electronic scanning," *Microwave J.*, Mar. 1996.
- [7] T. Mitsui, S. Nomura, and Landolt-Börnstein, "Numerical data and functional relationship in science and technology," *Ferroelectric Related Substances*, vol. 16, 1981.
- [8] Landolt-Börnstein, *Magnetic and Other Properties of Oxides and Related Compounds*, K.-H. Hellwege, Ed. New York, NY: Springer-Verlag, 1970, pt. b, vol. 4.
- [9] B. Lax and K. J. Button, *Microwave Ferrites and Ferrimagnetics*. New York, NY: McGraw-Hill, 1962.
- [10] H. How, "Magnetic microwave devices," in *Encyclopedia of Electrical and Electronics Engineering*, J. G. Webster, Ed. New York, NY: Wiley, 1999, vol. 12, pp. 31–45.
- [11] H. How, P. Shi, L. C. Kempel, K. D. Trott, and C. Vittoria, "Single-crystal YIG phase shifter using composite stripline structure at X -band," *J. Applied Phys.*, May 2000.
- [12] H. How, W. Tian, and C. Vittoria, "AC hall effect in multilayered semiconductors," *J. Lightwave Technol.*, vol. 15, no. 6, p. 1006, 1997.
- [13] C. Vittoria, *Microwave Properties of Magnetic Films*. New York: World Scientific, 1993.
- [14] F. L. Mesa, R. Marqués, and M. Horro, "A general algorithm for computing the bidimensional spectral Green's dyad in multilayered complex bianisotropic media: The equivalent boundary method," *IEEE Trans. Microwave Theory Tech.*, vol. 39, p. 1640, 1991.
- [15] E. El-Sharawy and R. W. Jackson, "Coplanar waveguide and slot line on magnetic substrates: Analysis and experiment," *IEEE Trans. Microwave Theory Tech.*, vol. 36, p. 1071, 1988.
- [16] M. Tsutsumi and T. Asahara, "Microstrip lines using yttrium iron garnet film," *IEEE Trans. Microwave Theory Tech.*, vol. 38, p. 1461, 1990.
- [17] H. How and C. Vittoria, "Microstrip antennas," in *Encyclopedia of Electrical and Electronics Engineering*, ser. Supplement, J. G. Webster, Ed. New York, NY: Wiley, Mar. 2000, vol. 25, pp. 61–78.

H. How, photograph and biography not available at time of publication.



Ping Shi received the B.S. degree in physics from Tsinghua University, Beijing, China, in 1996. He is currently pursuing the Ph.D. degree in electrical engineering in Northeastern University.

His current research interests include microwave and millimeter wave ferrite devices modeling, ferrite materials, MMIC ferrite device fabrication, thick film, and multilayer ceramics integrated circuit technology.

C. Vittoria, photograph and biography not available at time of publication.

E. Hokanson, photograph and biography not available at time of publication.

M. H. Champion, photograph and biography not available at time of publication.

Leo C. Kempel (S'89–M'94–SM'99) was born in Akron, OH, in October 1965. He received the B.S.E.E. degree from the University of Cincinnati in 1989 and participated in the cooperative education program at General Dynamics/Fort Worth Division. He received the M.S.E.E. and Ph.D. degrees from the University of Michigan, Ann Arbor, in 1990 and 1994, respectively.

After a brief post-doctoral appointment at the University of Michigan, he joined Mission Research Corporation in 1994 as a Senior Research Engineer. He led several projects involving the design of conformal antennas, computational electromagnetics, scattering analysis, and high power/ultrawideband microwaves. He joined Michigan State University as an Assistant Professor in 1998 where he is conducting research in computational electromagnetics and supervising the research of several M.S. and Ph.D. students. He recently co-authored the book *The Finite Element Method for Electromagnetics* (New York, NY: IEEE Press).

Dr. Kempel is serving as the Chapter IV Vice-Chair for the Southeast Michigan chapter of the IEEE as well as the vendor chair for the 2000 ACES Conference. He has organized several sessions at recent URSI and ACES meetings. He is an active reviewer for several IEEE publications as well as JEWA and *Radio Science* and a member of Tau Beta Pi, Eta Kappa Nu, and Commission B of URSI.



Keith D. Trott (S'84–M'86–SM'91) was born in Boston, MA on November 17, 1952. He received the B.S. degree in mathematics from SUNY, Plattsburgh in 1977, the M.S.E.E. degree from Syracuse University in 1981, and the Ph.D. degree from The Ohio State University in 1986, specializing in electromagnetic scattering and antennas.

He is currently Group Leader and Senior Research Engineer with MRC's Electromagnetic Applications Group in Valparaiso, FL where he conducts research in electromagnetic scattering, radar cross section, and computational electromagnetic methods to solve radiation and scattering problems. He is the Principal Investigator (PI) on several antenna and scattering projects. He has more than 30 publications. He has nearly 20 years experience in Air Force laboratories conducting research in radar cross-section phenomenology and electromagnetic scattering as it applies to the exploitation and modeling of basic radar target scattering physics. Before joining MRC, Dr. Trott was chief of the Munition Sensor Technology Branch at Wright Laboratory, Armament Directorate, Eglin Air Force Base FL and had also been the Senior Scientist for that branch. His current research interests include: phenomenology and modeling of the sensor/target interaction for both active and passive RF, bistatic RCS prediction techniques for conducting and material bodies, material parameter modeling and characterization, and computational electromagnetics to solve radiation and scattering problems. His awards include: Air Force Materiel Command Achievement Award for Science and Technology, Armament Directorate Senior Engineer of the Year, U.S. Air Force Research and Development Award, three Rome Lab Scientific Achievement Awards, Air Force Office of Scientific Research Star Team (member), and Rome Lab Research Team Award (member). His biography is listed in *Who's Who in Science and Engineering*.

Dr. Trott is a member of Sigma Xi and Eta Kappa Nu and has held an appointment as Adjunct Assistant Professor at AFIT.